Regular Article

Effect of Isopropanol on the Fluidization of Hydrophilic Titanium Nano-Powder

*H. Hoorijani, R. Zarghami, N. Mostoufi** *

Multiphase Systems Research Lab, School of Chemical Engineering, College of Engineering, University of Tehran, P. O. Box: 11155/4563, Tehran, Iran

ARTICLE INFO	ABSTRACT
	The effect of adding isopropanol (ISP) to nitrogen as the fluidizing gas on the hydrodynamics of the fluidization of hydrophilic titanium nanoparticles was studied. It was shown by the pressure drop method that adding ISP reduces the minimum fluidization velocity. Wavelet transform of the pressure fluctuations of the bed was employed to identify the hydrodynamic structures. The energy of hydrodynamic structures was evaluated in each fluidization mode. It was shown that ISP reduces the inter-particle attractive forces by replacing the hydroxyl group of the hydrophilic nanoparticles with an alkyl group. Energy and recurrence analyses were used to define the characteristics of fluidization when adding ISP to nitrogen gas. The energy of macro structures increased when using ISP, having indicated a decrease in the number of bubbles and an increase in the bubble size due to the reduction of inter-particle attractive forces. The increase of the white local areas in the recurrence plots also showed the increase of the bubble size. The recurrence quantification analysis showed the increase of the larger-scale phenomena (i.e. bubbles) in the bed.

1. Introduction

Nano-sized powders are recently being used in various industries [1]. Several applications, including fluidization, use nanoparticles (NPs) due to their high surface ratio, mass transfer, and heat transfer rates. There are two flow patterns in the fluidization of these powders [2, 3]: agglomerate particulate fluidization (APF) and agglomerate bubbling fluidization (ABF).

The APF flow regime has a uniform and high bed expansion while lower bed expansion and larger bubbles are the main characteristics of the ABF flow regime. Different internal and external assisting methods have been used to solve the difficulties associated with the fluidization of these powders or to improve their quality [4-7]. Among these methods, adding isopropanol (ISP) to the fluidizing gas

---

*Corresponding author: mostoufi@ut.ac.ir (N. Mostoufi)

is a well-suited method for improving the fluidization quality. Adding ISP to the fluidizing gas replaces the hydroxyl group of the hydrophilic particles with the alkyl groups of the ISP that have lower attractive force among particles which results in decreasing the size of agglomerates and improving the fluidization quality [8].

Tahmasebpour et al. [8] studied the effect of ISP on the surface of hydrophilic and hydrophobic NPs. Their results showed that ISP is absorbed on the surface of hydrophilic particles by forming hydrogen bonds. The alkyl groups of ISP molecules become then exposed on the surface of the hydrophilic titanium oxide NPs which exhibit lower attractive forces compared to the hydroxyl groups of the hydrophilic NPs. Tahmasebpour et al. [8] also investigated the effect of using ISP in the fluidizing gas on the hydrophobic NPs and reported a negative effect on the minimum fluidization velocity by increasing it for this type of powders. Vahdat et al. [9] investigated the effect of electric field on the fluidization of hydrophilic titanium oxide nanopowder. The hydrodynamics of the bed was studied by measuring the pressure drop and pressure fluctuations and reported that increasing the alternating electric field strength reduces the minimum fluidization velocity, bubble size, and agglomerates size. They also found that employing ISP increases the bed voidage at the minimum fluidization velocity. Liu and Wang [10] studied the effect of the initial height of the bed of NPs on the fluidization quality. They showed that the majority of the bed becomes fluidized at the bottom dense region under all fluidization conditions. Also, according to their findings, the size of agglomerates in the dilute region increases as the gas velocity and initial bed height are increased.

In the present study, the effect of adding ISP to the fluidizing gas on the hydrodynamics of the fluidization of hydrophilic titanium oxide NPs was investigated. Hydrodynamic structures (i.e., bubbles and agglomerates) in the bed were identified by the wavelet transform of pressure fluctuations. The recurrence analysis was used to investigate the effect of ISP on the quality and dynamic patterns of fluidization.
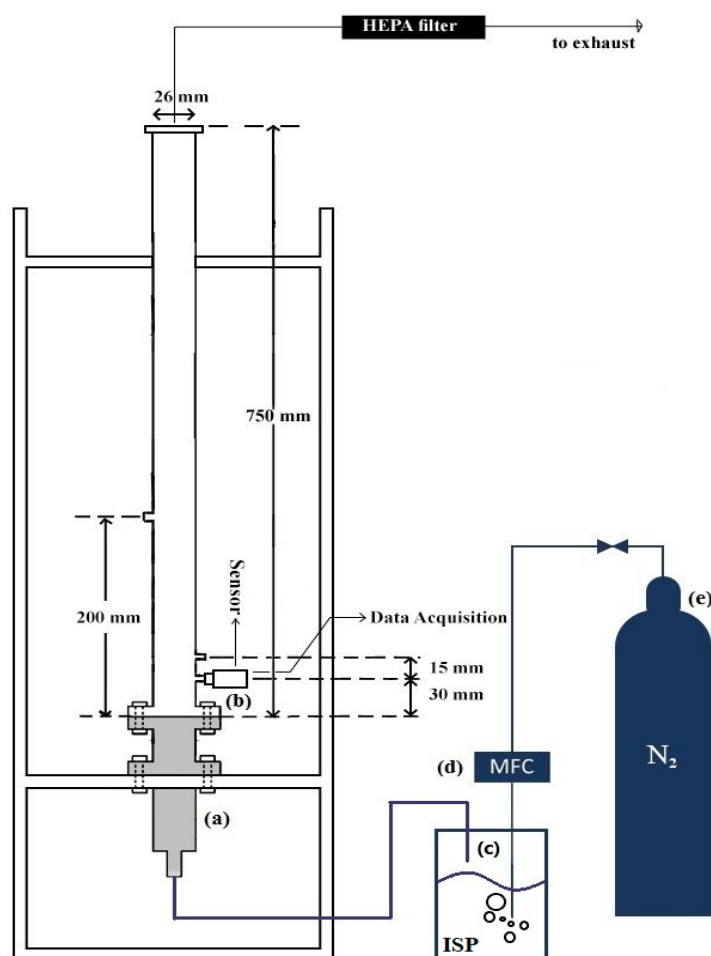
2. Experiments

A schematic of the experimental setup is shown in Figure 1. The fluidized bed was a cylindrical column of quartz with an inner diameter of 26 mm and a height of 800 mm. To ensure the perfect distribution of the inlet gas, a wind box and distributor plate were used under the column. The distributor plate was a sintered porous metal 316L SS, from MOTT Corp., Series 1100 with a porosity of 60 % and a thickness of 1 mm. Dry pure nitrogen was used as the fluidizing gas to prevent the effect of moisture and the liquid bridge force on the particles. To control and measure the flow rate of the gas, a digital mass flow controller (MC-5SLPM-D, Alicat Scientific, Inc., USA) was used. To mix the nitrogen with isopropanol (ISP), a bubbler with liquid ISP was used at the gas inlet to the bed. ISP was purchased from Merck (Germany). A high-efficiency particulate absorbing (HEPA) filter was used at the gas outlet of the column to prevent elutriation and the pollution of the environment.

AEROXIDE® TiO_2 P 25 with hydrophilic characteristics and a mean diameter of about 21 nm and a bulk density of 130 kg/m^3 was used in the experiments. In each test, 7 g of the powder was transferred into the column to reach the desired initial bed height of 6 cm. Certain steps were considered before fluidization: the powder was sieved using a

275 μm screen and a high flow rate of gas was applied into the bed to break the initial agglomerates formed during filling and

transportation. The regime of fluidization was ABF, with and without ISP.

Figure 1. Schematic of the experimental set-up of the (a) wind box (b) sampling ports and sensor (c) bubbler with ISP (d) mass flow controller (e) nitrogen supply tank.

The measurement of the pressure fluctuations of the bed was performed using a piezoresistive pressure sensor (model 7261, Kistler© Co., Switzerland). The sensor had a response time of less than 1 ms and an accuracy of 0.5 % of the full scale. The pressure drop of the bed was measured using a digital barometer (Cole Parmer, 1.0 in, WC). The piezoresistive sensor was placed at 25 mm above the distributor, and flush to the wall of the column. The sampling frequency of the

pressure signals was 400 Hz, satisfying the Nyquist criterion [11-13]. The pressure signal was filtered using a band-pass filter at a lower cut-off frequency of 0.1 Hz (to remove the bias value of the pressure) and an upper cut-off Nyquist frequency (100 Hz). Each experiment was repeated 3 times at atmospheric pressure and ambient temperature.

3. Data analysis
3.1. Wavelet transform

The wavelet transform decomposes a time series into a series of sub-signals, each representing different characteristics of the system. This transform uses a group of functions, $\psi_{jk}(t)$, that can be generated by adjusting the mother wavelet function $\psi(t)$ according to the following equation:

$$\psi_{jk}(t) = \frac{1}{\sqrt{|j|}} \sum_{i=1}^{N} \psi\left(\frac{t-k}{j}\right) \qquad (1)$$

Here, j and k are the parameters used to scale and translate the function $\psi(t)$ respectively. A detailed description of this method is reviewed in previous studies [6, 13, 14]. The sub-signals obtained from decomposition represent the main signal at different scales and resolutions. Therefore, their combination reconstructs the primary signal:

$$P'(i) \approx A_j(i) + \sum_{j=1}^{J} D_j(i) \qquad (2)$$

Here, j is the level of the orthogonal sub-signals, A_j and D_j are the two groups of approximation and detail sub-signals respectively. In this method, the energy of a signal P can be obtained from:

$$E = \sum_{i=1}^{N} |P(i)|^2 \qquad (3)$$

In the wavelet transform, choosing the proper mother wavelet and the level of decomposition are two important steps for the analysis [15]. In this work, the Daubechies mother wavelet was used and its order was determined by considering the minimum reconstruction error of the main signal. The reconstruction error is the difference between the primary signal (P) and the reconstructed one (P′). The suitable level of the

decomposition of the signal was determined through the analysis of the normalized Shannon entropy [16]. The decomposition level with the minimum Shannon entropy was considered the proper level of decomposition. In this study, the 2nd order Daubechies mother wavelet and 8th level of decomposition were used in the wavelet transform analysis.

3.2. Recurrence analysis

Researchers have adopted the recurrence analysis for analyzing nonlinear time series in the state space domain. Through this method, the disadvantages of other nonlinear analysis methods are eliminated by converting a multi-dimensional state space into a two-dimensional matrix of zeros and ones, as well as a plot corresponding to this matrix [17]. This plot, referred to as the recurrence plot (RP), provides a visual representation of the hydrodynamic state of the fluidized bed [14] by identifying the local white area (LWA) and local bold areas (LBA). LWA and LBA represent large and smaller phenomena respectively. It is possible to quantify the changes in the system using different parameters calculated from the recurrence matrix. The hydrodynamics of gas-solid fluidized beds of micro-sized particles was characterized by Tahmasebpour et al. [14] using the recurrence quantification analysis (RQA). They investigated the relationship between RQA parameters and the hydrodynamic status of the bed under various operating and design conditions. In another study, Tahmasebpour et al. [18] used the RQA and developed a novel approach based on the determinism of the decomposed pressure fluctuations to define the three main hydrodynamic structures (macro, meso, and micro) of fluidization. Using the recurrence analysis of pressure fluctuations and acoustic

emissions, Savari et al. [19] studied the effects of the particle size and bed diameter on the hydrodynamics of fluidization. According to their findings, an increase in the particle size results in a decrease in the recurrence rate, and adding larger particles to the bed enhances the effect of macrostructures.

3.2.1. Recurrence plots

The pressure fluctuations signal was normalized to reduce the effect of noises in the measurement system [20, 21]. In the recurrence analysis, the primary signal is converted into an m-dimensional state space trajectory as below:

$$\vec{z_i} = \sum_{k=1}^{d} x_{[i+(k-1)\tau]} \cdot \vec{e_k} \quad i = 1, 2, \dots, M, \quad M = N - (m-1)\tau \quad (4)$$

where $\vec{z_i}$, m, x, τ and $\vec{e_k}$ are the trajectory, the embedding dimension, the primary signal, the time delay, and the unit vector of the state space respectively. After obtaining the state space trajectory, the recurrence matrix, $R_{i,j}$, can be formed according to the following equation:

$$R_{i,j} = \Theta\left(\varepsilon - \|\vec{x_i} - \vec{x_j}\|\right) \quad i, j = 1, 2, 3, \dots, N \quad (5)$$

in which N is the number of state space points, $\vec{x_i}$, $\vec{x_j} \in R^m$ are the i-th and j-th components of the state space trajectory obtained, ε is a threshold distance, $\|.\|$ is the norm and $\Theta(.)$ is the Heaviside function. Based on equation (7), the norm of the distance between two different states of the trajectory at times I and j is calculated. This distance is then compared with the threshold distance to check if the two states are similar or not. At last, the Heaviside function returns 1 if the two compared states

are similar ($\varepsilon > \|\vec{x_i} - \vec{x_j}\|$, $R_{i,j}$=1), otherwise, if the states are not similar the Heaviside function returns 0 ($\varepsilon < \|\vec{x_i} - \vec{x_j}\|$, $R_{i,j}$=0) [22, 23]. To build the recurrence plots, the zero elements of the matrix are shown as white dots and black dots would appear for unity elements at the coordinate (I, j). The general pattern produced by these black and white dots on the RP represents the dynamics of the system. As mentioned earlier, the LWA on the RP represents high amplitude fluctuations which have values greater than the mean of the signals and the LBA are the high frequency and low amplitude fluctuations of the primary signal [24].

3.2.2. Recurrence quantification analysis

RPs are visual indicators of the dynamics of a system. To quantify the complexity and patterns of the RP, different parameters have been proposed in the literature which are known as the parameters of the recurrence quantification analysis (RQA) [22, 25]. Some of the RQA parameters considered in this study are described in this section. More detailed descriptions can be found in literatures and previous studies [18, 19, 26, 27].

The recurrence rate (RR) is a measure of the frequency of similar states occurring in a time series. The recurrence rate measures the change in the average size of agglomerates in fluidization.

$$RR = \frac{1}{N^2} \sum_{i,j=1}^{N} R_{i,j} \quad (6)$$

Determinism (DET) measures the predictability of a system. DET has a high value for periodic systems and low value for a stochastic system. In the NP fluidization, it is useful to determine the regime of fluidization

as well as the intensity of interactions between particle agglomerates.

$$DET = \frac{\sum_{l=l_{min}}^{N} lP(l)}{\sum_{l=1}^{N} lP(l)} \qquad (7)$$

Entropy (ENT) estimates the probability of the occurrence of a specific state that does not change (or changes slowly) over time. ENT measures the complexity of a fluidized bed and identifies the role of different hydrodynamic structures.

$$ENT = -\sum_{l=l_{min}}^{N} p(l)\ln(p(l)) \qquad (8)$$

Laminarity (LAM) measures the laminar state of the system. The intensity of interaction between agglomerates can be monitored using this parameter in fluidization.

$$LAM = \frac{\sum_{v=v_{min}}^{N} vP(v)}{\sum_{v=1}^{N} vP(v)} \qquad (9)$$

Trapping time (TT) means the time during which a system is trapped in a particular state. This helps to clarify the role of hydrodynamic structures.

$$TT = \frac{\sum_{v=v_{min}}^{N} vP(v)}{\sum_{v=v_{min}}^{N} P(v)} \qquad (10)$$

The average diagonal line length (L_{ave}) measures the average period during which a system is in a specific state at two different points in the trajectory. This method can be used to measure bubbles and observe the fluidization regime.

$$L_{ave} = \frac{\sum_{l=l_{min}}^{N} lP(l)}{\sum_{l=l_{min}}^{N} P(l)} \qquad (11)$$

In the above formulas, $P(l)$, $\sum lP(l)$, and l_{min} are the number of lines with the length of l, the black dots forming the diagonal lines and the minimal length of diagonal lines respectively. Babaei et al. [28] studied the effect of the minimal length of the line on RP and RQA and found ($l_{min} = 2$) to be the optimum choice as the lowest possible value to distinguish the different states of a system to study.

4. Results and discussion
4.1. Minimum fluidization velocity
The bed pressure drop against the superficial gas velocity for the two modes of fluidization (with and without ISP) are shown in Figure 2. The minimum fluidization velocity (U_{mf}) was determined based on this figure and given in Table 1. The flow regime of fluidization is also reported in this table. As it can be seen in this Table 1 and as also reported in previous studies [8], using ISP with the fluidizing gas reduces the minimum fluidization velocity while it does not affect the flow regime of the hydrophilic titanium oxide nanoparticles,. As explained by Tahmasebpour et al. [8], using ISP with the fluidizing gas causes the alkyl groups of ISP to bond with the hydroxyl groups of the nanoparticle using hydrogen bridges. The organic groups of ISP molecules become exposed on the surface of particles that exhibit lower attractive forces than the hydroxyl groups of the hydrophilic powder, reducing the chance of the formation of larger agglomerates. Consequently, smaller bubbles are formed and their number increases in the bed since the gas flows more easily through the dense phase of the powder. With the decrease of the attractive force between agglomerates, the agglomerate size decreases, and particles become fluidized at a lower gas velocity [9].
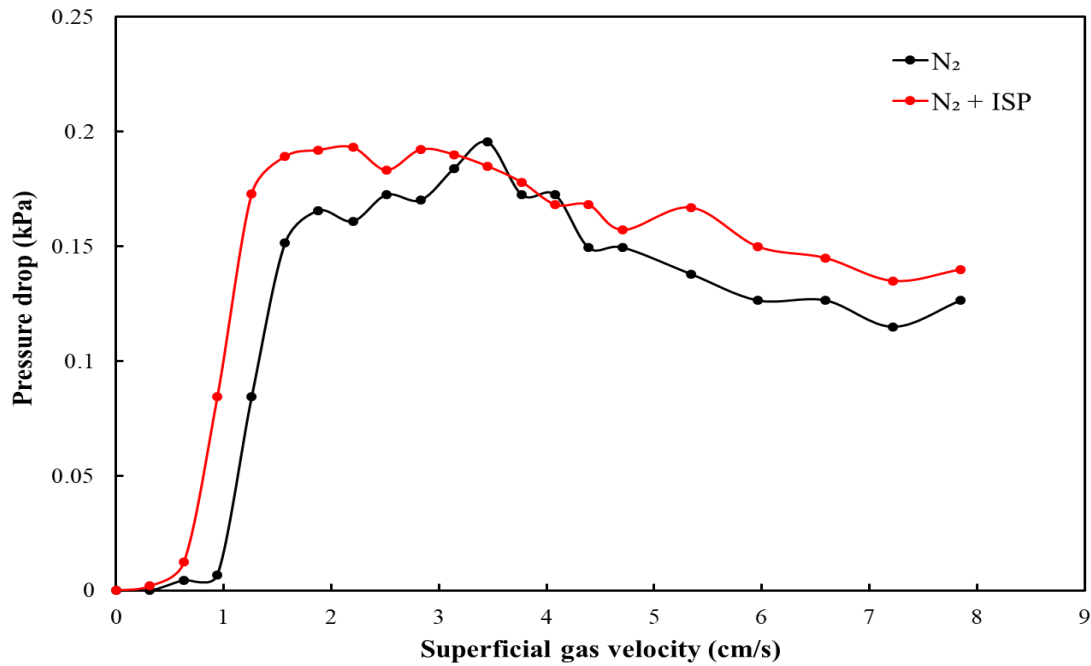
Figure 2. Pressure drop of the bed in fluidization with and without ISP at different superficial gas velocities.

Table 1
Characteristics of fluidization.

Fluidizing gas	Minimum fluidization velocity [cm/s]	Flow regime
N_2	1.5	ABF
N_2 + ISP	1.06	ABF

4.2. Wavelet transform

Figure 3 shows the determinism of the sub-signals for the fluidization with N_2 and N_2 + ISP as the fluidizing gas. Using the method proposed by Tahmasebpour et al. [14], the determinism was evaluated for the sub-signals to identify the hydrodynamic structures in the bed. As discussed earlier, the macrostructures are the large-scale phenomena in the bed which have low frequencies and high amplitudes. These phenomena have the highest determinism due to their low stochastic behavior. Mesostructures represent the agglomerates and it has been shown [11] that they include the higher frequencies in the power spectral density (PSD) analysis of the pressure signal. Therefore, in the evaluation of determinism, these structures include the sub-signals that have increasing trends of determinism. Microstructures present the noises of the measurement system in the nanoparticle fluidization. Due to the random nature of the noise, the sub-signals that form these structures have the smallest determinism. As there is no significant information about the hydrodynamics of the bed in microstructures, they were not separated from the mesostructures in this study and both are referred to as finer structures. The finer structure represents the chaotic behavior of nanoparticle agglomerates with the noises of the measurement system, and macro structure shows the larger phenomena (i.e., the movement of bubbles) in the bed.
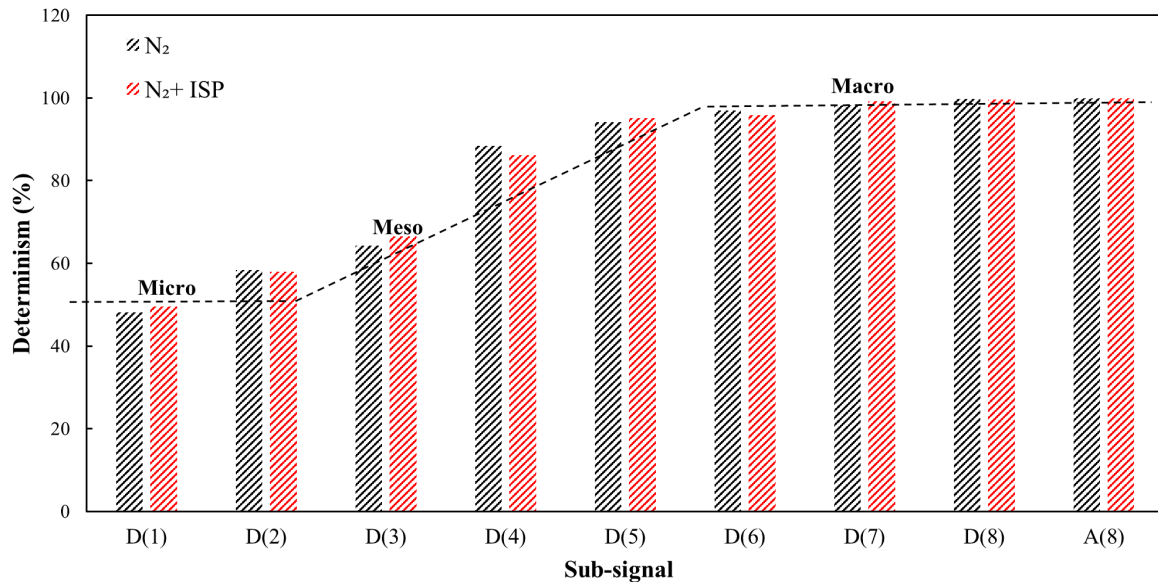
Figure 1. Determinism of sub-signals for different fluidization modes at a superficial gas velocity of 3.14 cm/s.

Figure 4 shows the energy analysis of the hydrodynamic structures for N_2 and N_2 + ISP as fluidizing gas at different gas velocities. The energy of each structure was calculated from equation (3). The contribution of each structure is the ratio of the energy of that structure over the total energy of the signal. As it can be seen in Figure 4(a), the energy contribution of the finer structures decreases by increasing the gas velocities. Also, adding ISP to the fluidizing gas decreases the energy contribution of finer structures and increases the contribution of macrostructures. As the attractive force of agglomerates decreases when using ISP, the size of agglomerates decreases in the bed in this case and decreases the energy contribution of the finer structures. The reduction of the energy contribution for the finer structures by increasing the gas velocity is due to the formation of more and larger bubbles in the bed which decreases the effect of agglomerates and their dynamic behavior. Based on the above discussions, the opposite trend can be seen in Figure 4(b) for the energy contribution of macrostructures (bubbles).
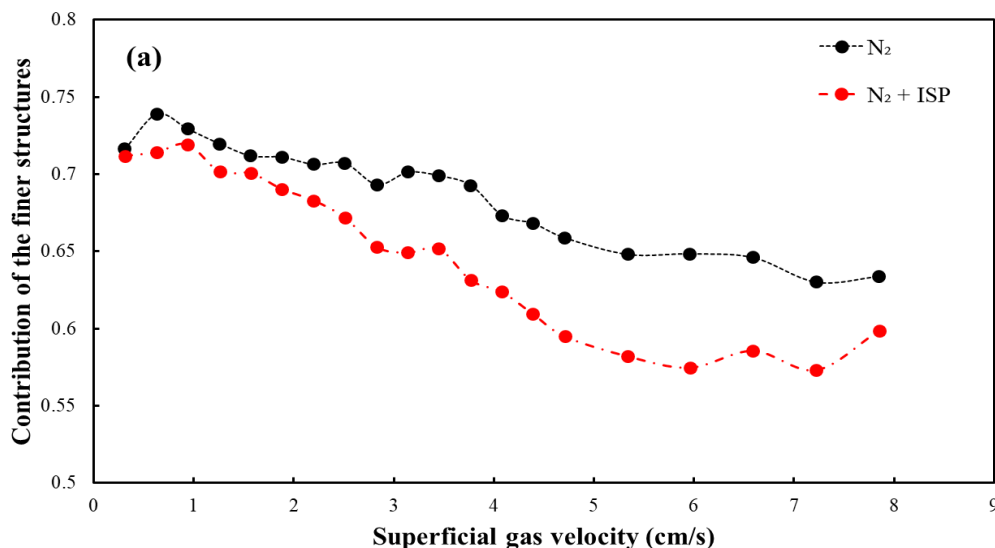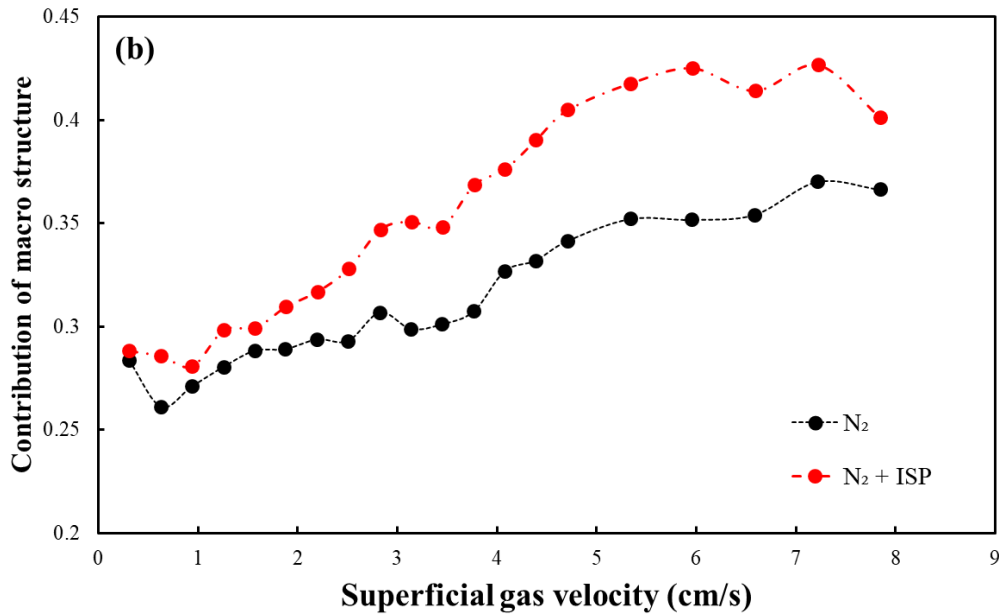
Figure 2. Energy contribution of the hydrodynamic structures for a bed fluidized with and without ISP at different gas velocities (a) Finer structures (b) Macro structures.

To better investigate the effect of adding ISP to the fluidizing gas, the energy contribution of each hydrodynamic structure at the superficial gas velocity of 3.14 cm/s is shown in Figure 5. As it can be seen in this figure, fluidizing the bed with N_2 + ISP reduces the energy contribution of the mesostructures and increases the contribution of macrostructures. The attractive force between the agglomerates becomes lower in this case which results in the formation of larger bubbles. This figure also indicates that adding ISP has no meaningful effect on the energy contribution of the microstructures.
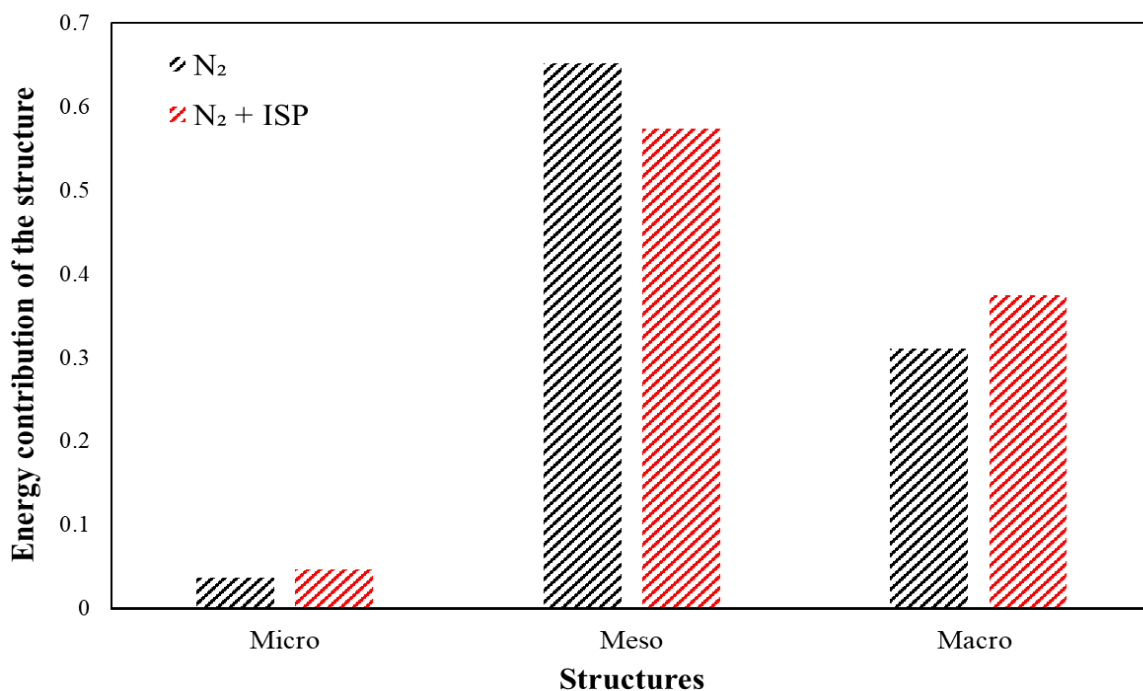

Figure 5. Energy analysis of hydrodynamic structures for the bed fluidized with and without adding ISP to the fluidizing gas. The superficial gas velocity is 3.14 cm/s.

**4.3. Recurrence analysis**

4.3.1. Recurrence Plot (RP)

The recurrence plots of the two fluidization modes of N2 + ISP and N2 as the fluidizing gas are shown in Figure 6 at a superficial gas velocity of 3.14 cm/s. These plots were constructed using the embedding dimension, time delay, minimum diagonal line, and vertical line of 2, 1, 2, and 2 respectively [28]. The radius threshold for the recurrence analysis was determined using the method proposed by Webber and Ziburt [26]. Five seconds of the pressure fluctuations signal were employed for the construction of these

plots. The LWA in the RP corresponds to the large-scale phenomena in the bed (bubbles) or low-frequency peaks with a high amplitude of the signal. The LBA is high-frequency fluctuations of the signal which come from the small-scale phenomena (agglomerates) of the fluidization. As it can be seen in Figure 6, using N2 + ISP increases the LWA which indicates the increase of the bubble size in the bed. As discussed in the previous section, the attractive force among agglomerates decreases when using ISP which results in the formation of smaller agglomerates, that can be seen by the decrease of the LBA in the RP.

(a)

(b)
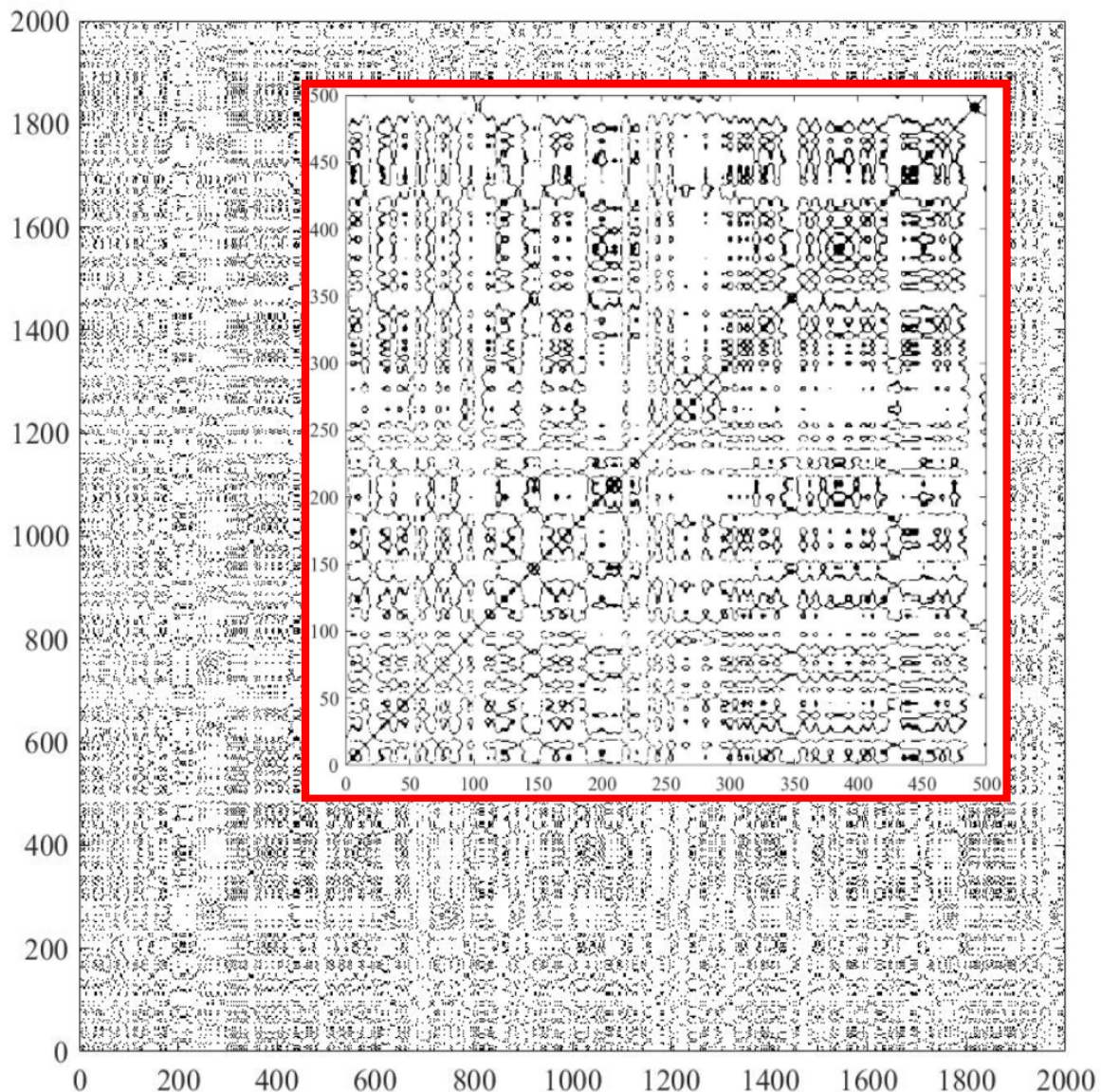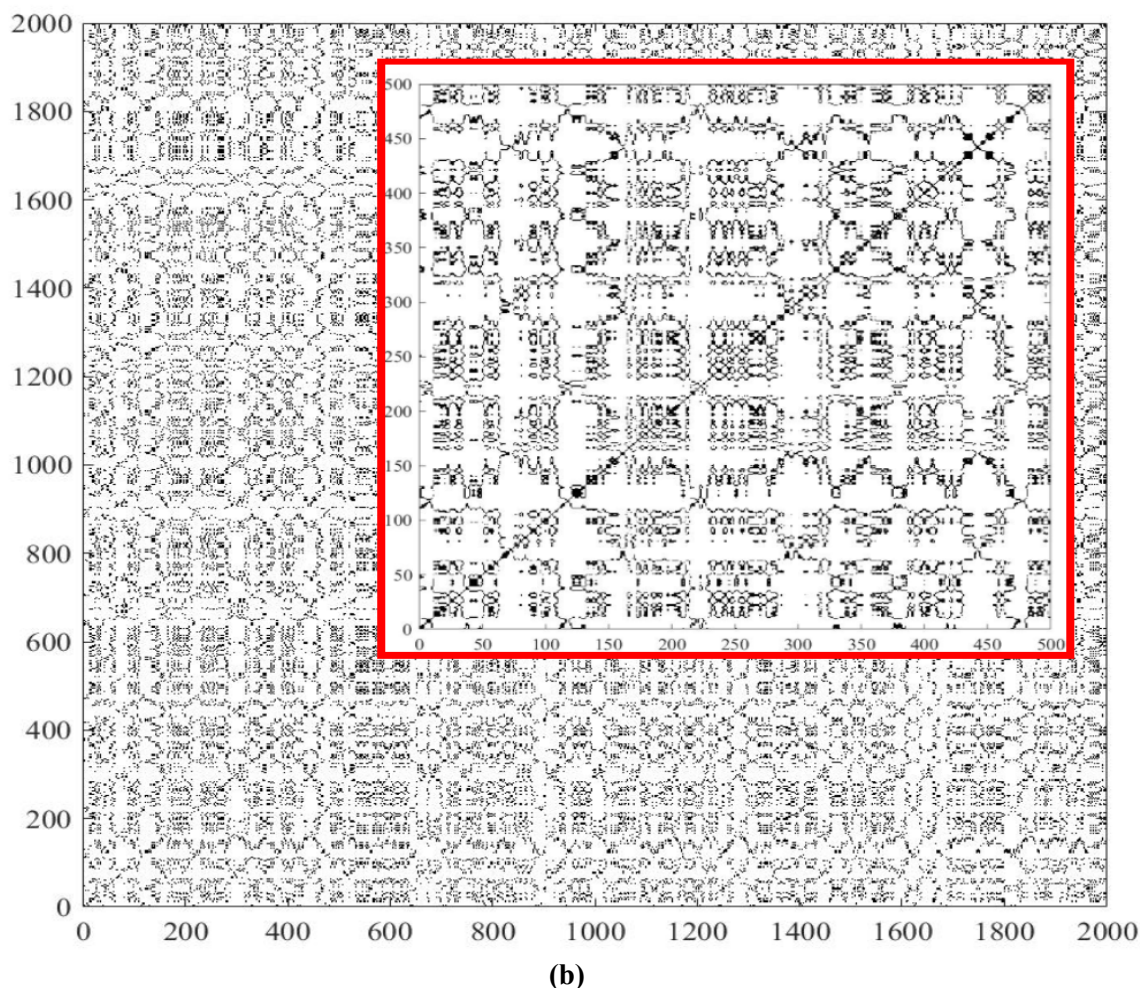
Figure 6. Recurrence plots of the fluidization at the superficial gas velocity of 3.14 cm/s (the embedding dimension of 2, time delay of 1, radius threshold of 0.23 and minimal diagonal and line length of 2) (a) N_2 (b) N_2 + ISP.

4.3.2. Recurrence quantification analysis (RQA)

Figure 7 shows the RQA parameters at various superficial gas velocities for the bed fluidized with N_2 + ISP and N_2. Figure 7(a) shows the recurrence rate at different gas velocities. The recurrence rate quantifies the number of recurrence states of the system by considering the ones and zeros of the recurrence matrix. In fluidization, this parameter can be related to the average particle size as mentioned by Savari et al. [19]. In the NP fluidization, agglomerates have the dynamic behavior of continuous merger and breakage and during the process their average size does not have a constant value. This trend has been observed in

previous studies as well [6] and RR has had no significant information regarding the hydrodynamics of the NP fluidization.

The determinism at different gas velocities is shown in Figure 7(b). As it can be seen in this figure, the determinism is higher for N_2 + ISP compared to when only N_2 is used as the fluidizing gas. Also, by increasing the gas velocity, the determinism increases in both cases. The ISP molecules expose the surface of hydrophilic titanium oxide NPs with the alkyl group, as discussed previously. These groups have a weaker attractive force than the hydroxyl groups, hence result in the formation of smaller agglomerates during the process and increase the bed voidage by forming larger

bubbles. Also, by increasing the gas flow into the bed, bubbles grow larger. As bubbles are the large phenomena in the NP fluidization, they have the largest deterministic value in the process. Consequently, the determinism increases by increasing the gas velocity, as it can be seen in Figure 7(b).

The variation of entropy with the gas velocity for both modes of fluidization is shown in Figure 7(c). This figure shows that using N_2 + ISP increases the entropy at high gas velocities compared to N_2. Also, increasing the gas velocity elevates the value of entropy for both modes of fluidization. Entropy measures the probability of a specific state reoccurring during the process and in the pressure signal. As there are more bubbles for N_2 + ISP, there is the probability of observing the same size bubbles during the process. This trend suggests that using ISP increases the periodic behavior of fluidization by weakening the attractive force between the agglomerates.
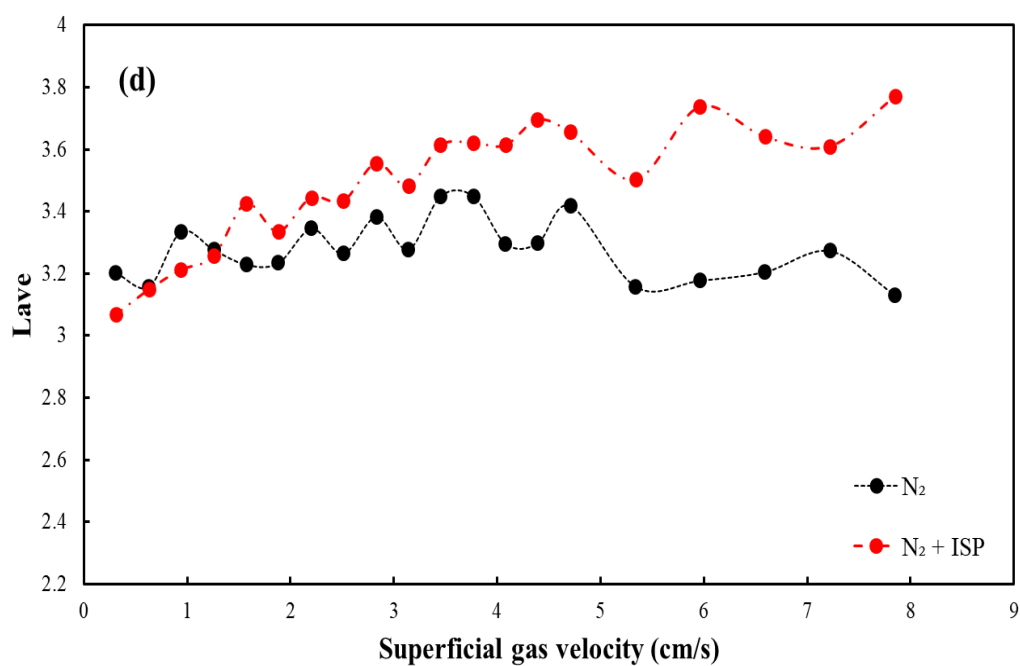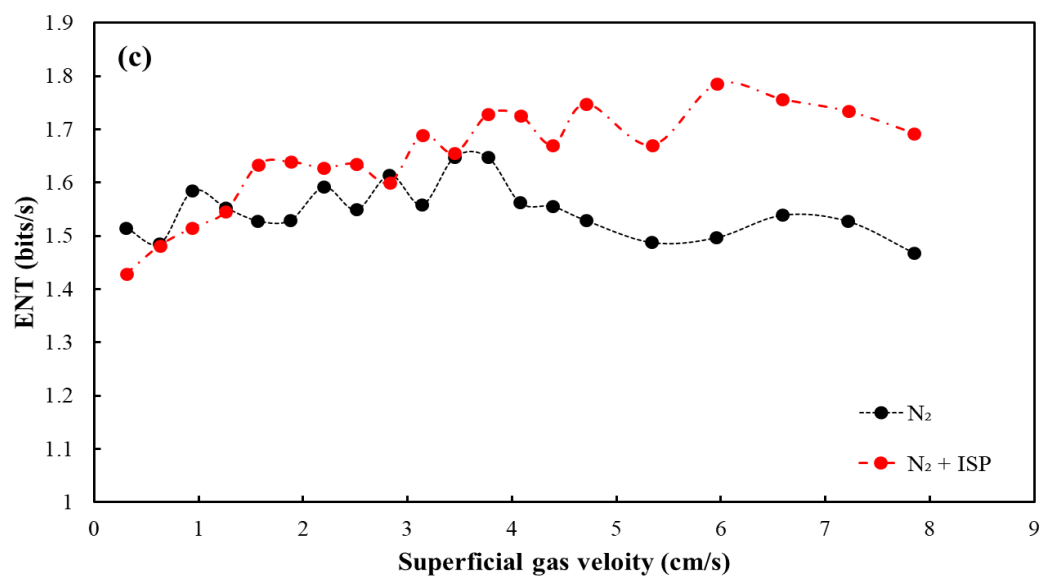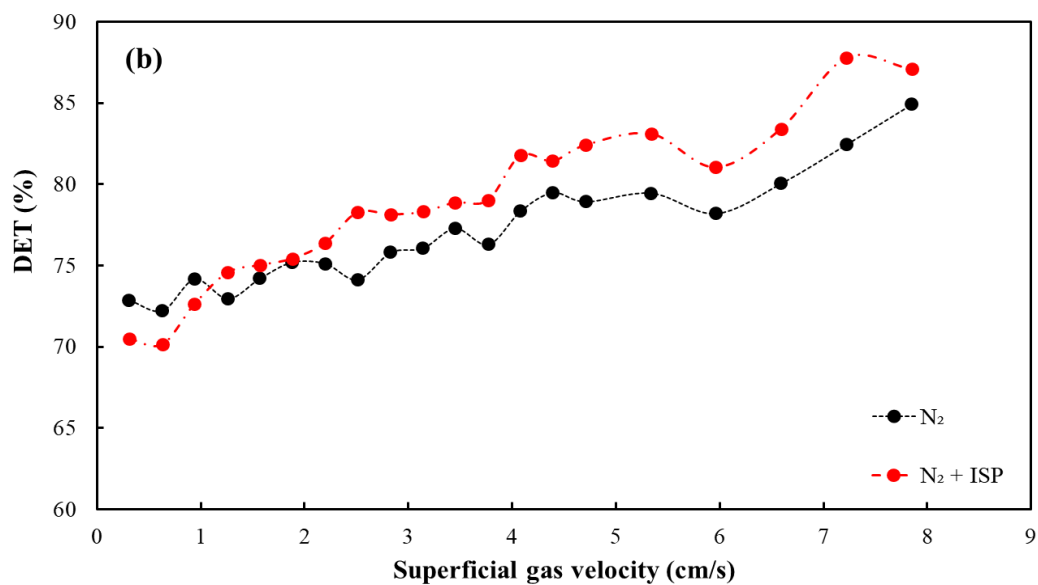
The evaluation of the average length of diagonal lines at different gas velocities is shown in Figure 7(d) for N_2 + ISP and N_2 as the fluidizing gas. As it can be seen in this figure, using ISP and increasing the gas velocity increase the average diagonal line length. The average length of diagonal lines increases when the bubbles grow in the bed.

This parameter measures the average time that the system stays at a specific state at two different parts of the signal. As the size of the bubbles increases in the bed, as discussed in Figure 7(b), the recurring of a specific state increases in the pressure signal.

Figure 7(e) shows the evaluation of laminarity against the superficial gas velocity for the two modes of fluidization. It can be seen in this figure that the laminarity is higher when using ISP with the fluidizing gas. Also, this parameter increases by increasing the superficial gas velocity. An increase in the contribution of macrostructure, as explained in Figures (4) and (5) for N_2 + ISP, causes the period when the bed stays in laminar states to increase due to the deterministic behavior of the bubbles.

Changes in trapping time at various gas velocities are presented in Figure 7(f) for the two modes of fluidization. As it can be seen in this figure, adding ISP to the fluidizing gas increases the trapping time. Also, the trapping time increases by increasing the gas velocity. When using ISP with the fluidizing gas, the contribution of macrostructure in the bed increases, and the bubbles become larger, the stochastic pattern during fluidization becomes lower and the trapping time increases.
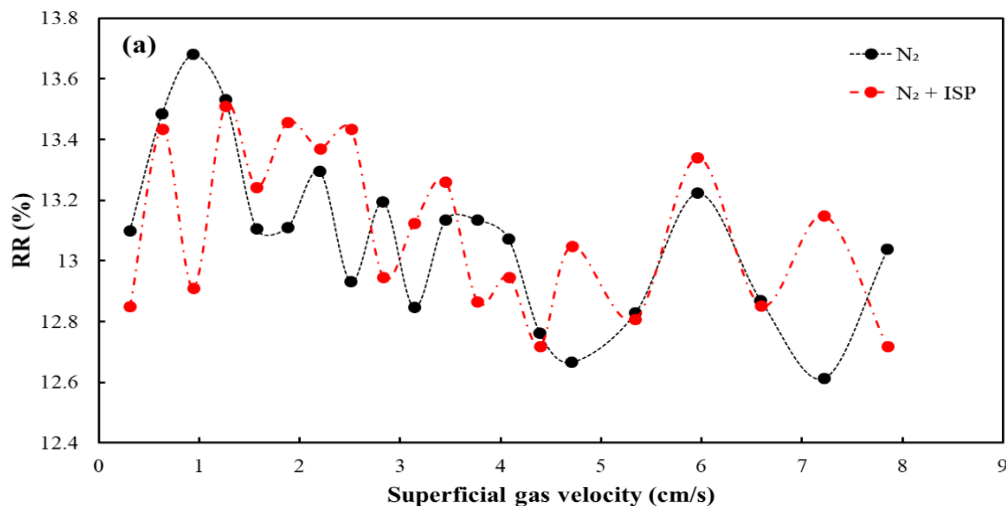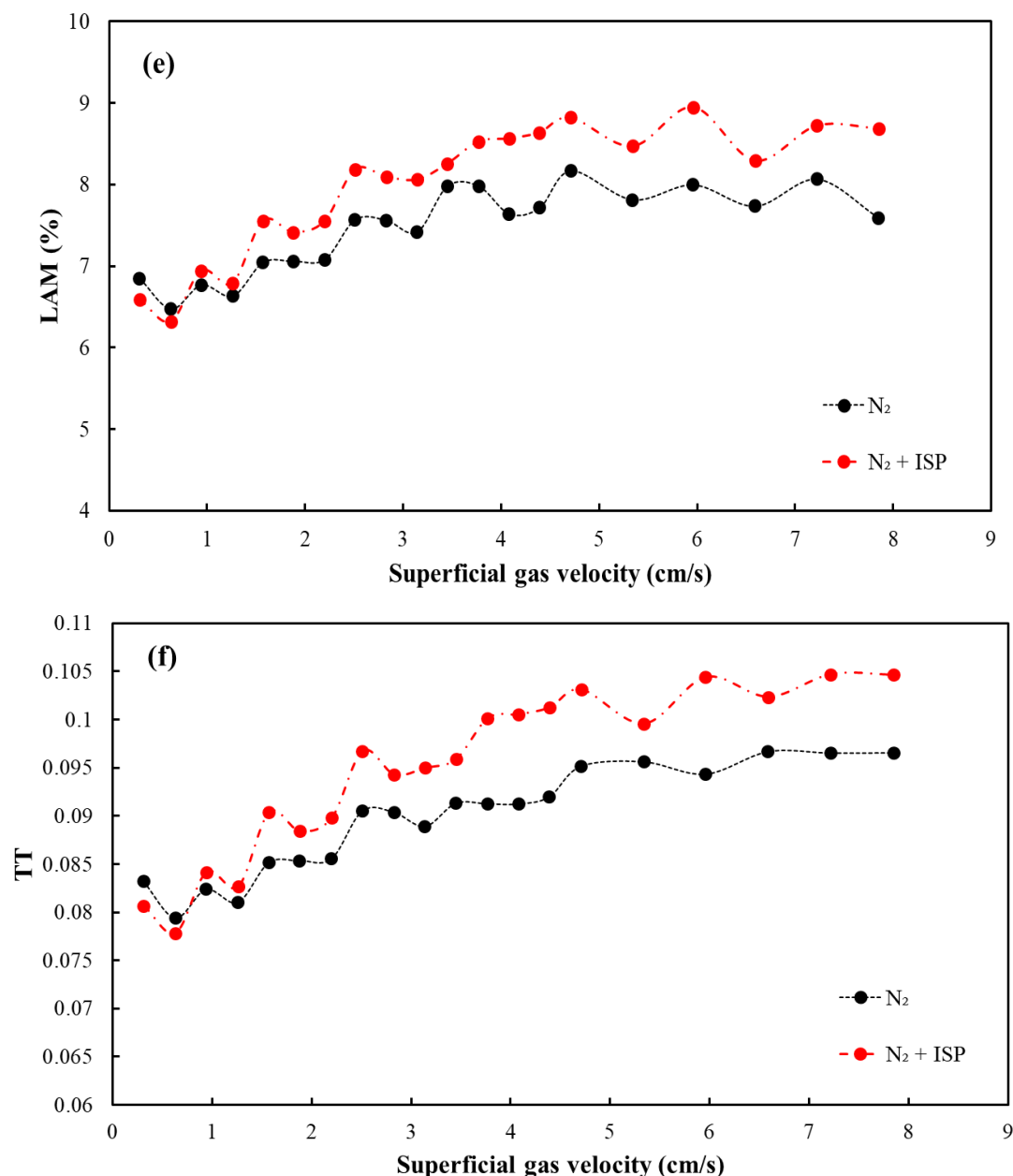
Figure 7. RQA parameters of the fluidization at different superficial gas velocities for both fluidization modes, (a) The recurrence rate, (b) Determinism, (c) Entropy, (d) The average length of diagonal lines, (e) Laminarity, (f) The trapping time.

5. Conclusions

The hydrodynamic characteristics of the fluidization of hydrophilic titanium oxide NPs when using isopropanol with nitrogen (ISP + N_2) as fluidizing gas were studied. The effect of ISP on fluidization was investigated by recording and analyzing pressure fluctuations using wavelet and recurrence analyses. The changes in the different hydrodynamic phenomena of the bed were evaluated by measuring the energy contribution of various hydrodynamic structures in the bed (finer and macrostructures). The results of energy and recurrence analyses indicated that adding ISP reduces the attractive force between particles and prevents the formation of larger agglomerates. Also, ISP reduces the minimum fluidization velocity and agglomerate size in the bed.

The energy analysis of the hydrodynamic

structures showed that the ISP increases the contribution of the macrostructure (i.e., bubbles) in the bed. The ISP having the increasing effect on the size and the decreasing effect on the number of bubbles was also noted in the recurrence plots through increasing the large white areas. ISP covers the hydroxyl groups of hydrophilic titanium oxide with alkyl groups that exhibit a lower attractive force. This phenomenon also causes an increase in the voidage in the bed and bubbles. RQA was performed using ISP + N_2 as the fluidizing gas. The results of this analysis revealed that ISP reduces the minimum fluidization velocity and the attractive force of the particle agglomerates of hydrophilic titanium nanoparticles. Moreover, ISP increases the bubble size in the bed by lowering the attractive force of the particles and increases the RQA parameters.

Nomenclature

$A_j(i)$	approximate sub-signal.
$D_j(i)$	detail sub-signal.
DET	determinism.
E	energy of signal [Pa^2/Hz].
E_j^A	energy of approximatie signal [Pa^2/Hz].
E_j^D	energy of detail signal [Pa^2/Hz].
ENT	entropy.
j	index for rescale in wavelet transform.
k	index for shift in wavelet transform.
l	diagonal line length.
l_s	segment length.
L_{ave}	average diagonal line length.
LAM	laminarity.
m	embedding dimension.
$P(i)$	measured pressure signal [Pa].
N	number of data points.
N_l	number of diagonal lines.
$P(l)$	number of diagonal lines of length *l*.
$P(v)$	number of vertical lines of length v.
$P'(i)$	reconstructed signal.
$R_{i,j}$	recurrence plot matrix.
TT	trapping time.
U	superficial gas velocity [m/s].
$\psi(t)$	mother wavelet function.
U_{mf}	minimum fluidization velocity [m/s].
$\vec{y_1}$	i-th point of state space trajectory.

Greek letters

ε	radius threshold.
Θ	Heaviside function.
υ	vertical line length.
τ	time delay vector.

References

[1] van Ommen, J. R., Valverde, J. M. and Pfeffer, R., "Fluidization of nanopowders: A review", *Journal of Nanoparticle Research*, **14** (3), 1 (2012).

[2] Yao, W., Guangsheng, G., Fei, W. and Jun, W., "Fluidization and agglomerate structure of SiO_2 nanoparticles", *Powder Technology*, **124** (1-2), 152 (2002).

[3] Liu, Y., Ohara, H. and Tsutsumi, A., "Pulsation-assisted fluidized bed for the fluidization of easily agglomerated particles with wide size distributions", *Powder Technology*, **316**, 388 (2017).

[4] Valverde, J. M. and Castellanos, A., "Effect of vibration on agglomerate particulate fluidization", *AIChE Journal*, **52** (5), 1705 (2006).

[5] An, K. and Andino, J. M., "Enhanced fluidization of nanosized TiO_2 by a microjet and vibration assisted (MVA) method", *Powder Technology*, **356**, 200 (2019).

[6] Hoorijani, H., Zarghami, R., Nosrati, K. and Mostoufi, N., "Investigating the hydrodynamics of vibro-fluidized bed of hydrophilic titanium nanoparticles", *Chemical Engineering Research and Design*, **174**, 486 (2021).

[7] Zhao, Z., Liu, D., Ma, J. and Chen, X., "Fluidization of nanoparticle agglomerates assisted by combining vibration and stirring methods", *Chemical Engineering Journal*, **388**, 124213 (2020).

[8] Tahmasebpoor, M., de Martín, L., Talebi, M., Mostoufi, N. and van Ommen, J. R.,

"The role of the hydrogen bond in dense nanoparticle–gas suspensions", *Physical Chemistry Chemical Physics*, **15** (16), 5788 (2013).

[9] Vahdat, M. T., Zarghami, R. and Mostoufi, N., "Fluidization characterization of nano-powders in the presence of electrical field", *The Canadian Journal of Chemical Engineering*, **96** (5), 1109 (2018).

[10] Liu, H. and Wang, S., "Fluidization behaviors of nanoparticle agglomerates with high initial bed heights", *Powder Technology*, **388**, 122 (2021).

[11] Tamadondar, M. R., Zarghami, R., Tahmasebpoor, M. and Mostoufi, N., "Characterization of the bubbling fluidization of nanoparticles", *Particuology*, **16**, 75 (2014).

[12] Esmailpour, A. A., Mostoufi, N. and Zarghami, R., "Effect of temperature on fluidization of hydrophilic and hydrophobic nanoparticle agglomerates", *Experimental Thermal and Fluid Science*, **96**, 63 (2018).

[13] Karimi, F., Haghshenasfard, M., Sotudeh-Gharebagh, R., Zarghami, R. and Mostoufi, N., "Enhancing the fluidization quality of nanoparticles using external fields", *Advanced Powder Technology*, **29** (12), 3145 (2018).

[14] Tahmasebpoor, M., Zarghami, R., Sotudeh-Gharebagh, R. and Mostoufi, N., "Characterization of fluidized beds hydrodynamics by recurrence quantification analysis and wavelet transform", *International Journal of Multiphase Flow*, **69**, 31 (2015).

[15] Rodrigues, A. P., D'Mello, G. and Srinivasa Pai, P., "Selection of mother wavelet for wavelet analysis of vibration signals in machining", *Journal of Mechanical Engineering and Automation*, **6** (5A), 81 (2016).

[16] Rioul, O. and Vetterli, M., "Wavelets and signal processing", *IEEE Signal Processing Magazine*, **8** (4), 14 (1991).

[17] Ziaei-Halimejani, H., Zarghami, R. and Mostoufi, N., "Investigation of hydrodynamics of gas-solid fluidized beds using cross recurrence quantification analysis", *Advanced Powder Technology*, **28** (4), 1237 (2017).

[18] Tahmasebpour, M., Zarghami, R., Sotudeh-Gharebagh, R. and Mostoufi, N., "Characterization of various structures in gas-solid fluidized beds by recurrence quantification analysis", *Particuology*, **11** (6), 647 (2013).

[19] Savari, C., Sotudeh-Gharebagh, R., Zarghami, R. and Mostoufi, N., "Non-intrusive characterization of particle size changes in fluidized beds using recurrence plots", *AIChE Journal*, **62** (10), 3547 (2016).

[20] Babaei, B., Zarghami, R. and Sotudeh-Gharebagh, R., "Monitoring of fluidized beds hydrodynamics using recurrence quantification analysis", *AIChE Journal*, **59** (2) 399 (2013).

[21] van Ommen, J. R., Coppens, M. O., van den Bleek, C. M. and Schouten, J. C., "Early warning of agglomeration in fluidized beds by attractor comparison", *AIChE Journal*, **46** (11), 2183 (2000).

[22] Marwan, N., Romano, M. C., Thiel, M. and Kurths, J., "Recurrence plots for the analysis of complex systems", *Physics Reports*, **438** (5-6), 237 (2007).

[23] Eckmann, J. -P., Kamphorst, S. O. and Ruelle, D., "Recurrence plots of dynamical systems", *World Scientific Series on Nonlinear Science Series A*, **16**, 441 (1995).

[24] Tahmasebpour, M., Zarghami, R., Sotudeh-Gharebagh, R. and Mostoufi, N., "Study of transition velocity from bubbling to turbulent fluidisation by recurrence plots analysis on pressure fluctuations", *The Canadian Journal of Chemical Engineering*, **91** (2), 368 (2013).

[25] Marwan, N., "A historical review of recurrence plots", *The European Physical Journal Special Topics*, **164** (1), 3 (2008).

[26] Webber Jr, C. L. and Zbilut, J. P., "Dynamical assessment of physiological systems and states using recurrence plot strategies", *Journal of Applied Physiology*, **76** (2), 965 (1994).

[27] Savari, C., Kulah, G., Sotudeh-Gharebagh, R., Mostoufi, N. and Koksal, M., "Early detection of agglomeration in conical spouted beds using recurrence plots", *Industrial & Engineering Chemistry Research*, **55** (26), 7179 (2016).

[28] Babaei, B., Zarghami, R., Sedighikamal, H., Sotudeh-Gharebagh, R. and Mostoufi, N., "Selection of minimal length of line in recurrence quantification analysis", *Physica A: Statistical Mechanics and its Applications*, **395**, 112 (2014).